



Freezing point depression and freeze-thaw damage by nanofluidic salt trapping

Tingtao Zhou ^{*}

Department of Physics, Massachusetts Institute of Technology, Cambridge, Massachusetts 02139, USA

Mohammad Mirzadeh

*Department of Chemical Engineering, Massachusetts Institute of Technology, Cambridge,
Massachusetts 02139, USA*

Roland J.-M. Pellenq [Ⓛ]

*The MIT/CNRS/Aix-Marseille University Joint Laboratory, “Multi-Scale Materials Science for Energy
and Environment,” and Department of Civil and Environmental Engineering, Massachusetts Institute
of Technology, Cambridge, Massachusetts 02139, USA*

Martin Z. Bazant[†]

*Department of Chemical Engineering and Department of Mathematics, Cambridge,
Massachusetts 02139, USA*



(Received 28 July 2020; accepted 9 November 2020; published 2 December 2020)

A remarkable variety of organisms and wet materials are able to endure temperatures far below the freezing point of bulk water. Cryotolerance in biology is usually attributed to “antifreeze” proteins, and yet massive supercooling ($< -40^{\circ}\text{C}$) is also possible in porous media containing only simple aqueous electrolytes. For concrete pavements, the common wisdom is that freeze-thaw (FT) damage results from the expansion of water upon freezing, but this cannot explain the high pressures (> 10 MPa) required to damage concrete, the observed correlation between pavement damage and deicing salts, or the FT damage of cement paste loaded with benzene (which contracts upon freezing). In this work, we propose a different mechanism—nanofluidic salt trapping—which can explain the observations, using simple mathematical models of dissolved ions confined between growing ice and charged pore surfaces. When the transport time scale for ions through charged pore space is prolonged, ice formation in confined pores causes enormous disjoining pressures via the ions rejected from the ice core, until their removal by precipitation or surface adsorption at lower temperatures releases the pressure and allows complete freezing. The theory is able to predict the nonmonotonic salt-concentration dependence of FT damage in concrete and provides some hint to better understand the origins of cryotolerance from a physical chemistry perspective.

DOI: [10.1103/PhysRevFluids.5.124201](https://doi.org/10.1103/PhysRevFluids.5.124201)

^{*}Present address: Division of Engineering and Applied Sciences, California Institute of Technology, Pasadena, California 91125, USA; edmondztt@gmail.com

[†]bazant@mit.edu

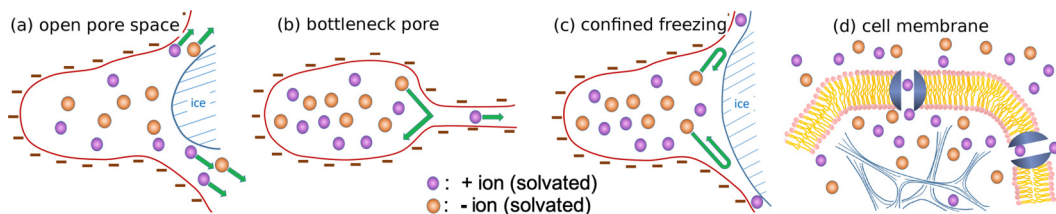


FIG. 1. Physical picture of nanofluidic salt trapping. (a) In an open pore, where ions and water molecules can easily exchange with a nearby reservoir, no significant pressure or freezing point depression is predicted. (b) Nanoscale bottlenecks, especially in poorly connected porous networks, with charged surfaces can significantly hinder this exchange by size or charge exclusion of the co-ions, and counterions are forced to stay to maintain charge neutrality. (c) Once ice nucleates, even an initially open pore will eventually trap a nanoscale thin film of supercooled, concentrated electrolyte near the charged surface, until surface ion condensation or solid salt precipitation occurs. (d) In biological cells, the charged cytoskeleton (indicated by fibers) could enable such passive nanofluidic salt trapping, while further active control of water and ion flux across the cell membrane is performed by ion channels and pumps. In all cases, nanofluidic salt trapping can lead to dramatic supercooling and, once ice nucleates, severe damage to the solid matrix.

I. INTRODUCTION

The durability of wet porous materials against freeze-thaw (FT) damage is critical in many areas of science and engineering. In biology, it is a matter of life and death. Living cells must somehow maintain a liquid state within the cellular membrane during winter [1–3], while avoiding anoxia due to external ice encasement [4]. Various antifreeze proteins have been identified in cryotolerant animals, and cryoprotectant chemicals have been used for cryopreservation and *in vitro* fertilization [2,5–7]. In addition, the complex thermodynamics of supercooled water could play a role. Even in bulk water, deep supercooling can lead to multiple metastable disordered states [8–10]. Phase transitions under nanoconfinement [11,12] can lead to exotic new phases, as well as modified ice nucleation, in both experiments [13–15] and molecular simulations [16,17] of water in nanopores.

In engineering, the most familiar example of FT damage is the fracture of concrete pavements during the winter [18], commonly attributed to the expansion of water transforming to ice within the pores [19,20]. However, this contradicts the observation that FT damage occurs when cement is loaded with benzene [21], a normal liquid that shrinks upon freezing. Recent experiments have challenged the prevailing hypothesis that FT damage is directly caused by solid phase transformations, not only ice formation [18,19], but also salt crystallization [22,23]. Interestingly, there is a strong correlation between FT damage and the use of deicing salts on concrete pavements [24], which are often less durable than concrete structures without salt exposure in the same cold climates. Moreover, FT damage only occurs when the water saturation level exceeds a critical value [25]. Previous models of “frost heave” (see, e.g., Ref. [26]) achieved some successes in explaining the deformation of saturated soils due to the dynamics of premelted liquid and its coupling with the solid. However, the applicability of these theories to hardened cement is questionable, due to its much higher stiffness compared to capillary stresses [27,28]. In summary, despite the societal importance of FT damage in cement, a physics-based theory has not yet been developed that can predict the enormous pressures required (>10 MPa), as well as all puzzling observations above.

In this article, we develop a predictive theory of freezing point depression and FT damage in charged porous media, based on a simple new mechanism sketched in Fig. 1: nanofluidic salt trapping. It is well known in colloid science that when two charged surfaces are separated by a liquid electrolyte, the crowding of ions in solution results in large repulsive forces whenever the electric double layers overlap, at the scale of the Debye screening length (1–100 nm in water). This “disjoining pressure” is responsible for the stabilization of colloidal dispersions in aqueous electrolytes [29], surface forces in clays and other porous media [30], and electrostatic properties

of membranes [31]. Disjoining pressure has been successfully modeled by the Poisson-Boltzmann (PB) mean-field theory for solutions of monovalent ions, and extensions are available to describe correlation effects involving multivalent ions [32,33]. Here we treat the disjoining pressure between the ice core and the charge pore surface with a mean-field approximation. Although the physics of electrolyte freezing under confinement has been considered for nanoporous materials [34], we propose that nanofluidic salt trapping is the key mechanism for large supercooling and FT damage in cement and other charged nanoporous materials. This physical picture is consistent with all the available experimental evidence for concrete.

A. Physical picture

Consider a heterogeneous porous material saturated with liquid and subjected to continuously decreasing temperatures. As in most organisms and construction materials, suppose that the pore surfaces and suspended materials are hydrophilic and charged [35–41], e.g., by the dissociation of surface functional groups or the adsorption of charged species. The large capillary pores (>5 nm) are typically also filled with water but can be replaced with other fluids such as benzene. However, the small “gel” pores (~ 1 – 5 nm) are always filled with liquid water due to the strong surface charge and hydrophilicity even in benzene-loaded cement samples. Importantly, the liquid must contain dissolved salts, possibly at a low concentration, as well as excess counterions to screen the pore surface charges and preserve overall electroneutrality. Ions in solution mediate surface forces [30], which play a crucial role in the mechanical properties of concrete [32,33,42–45] and the function of biological systems. In most cases, the ions are assumed to have negligible solubility in the frozen solid, as is the case with pure ice.

Freezing begins in the larger “macropores” (>100 nm), where bulk water easily transforms to ice, slightly below the thermodynamic melting point of the solution, which may be depressed from that of the pure solvent by the dissolved salt and any antifreeze solutes. This bulk ice can form by homogeneous nucleation, spinodal decomposition, or (most likely) heterogeneous nucleation on impurities. Regardless of its origin, the advancing ice rejects ions, causing the salt concentration to rise in the nearby, increasingly confined liquid electrolyte.

What happens next depends on the degree of supercooling, the surface charge, and, importantly, the pore connectivity. As shown in Fig. 1(a), even after partial freezing, an individual pore may remain open, allowing ions and water molecules to exchange freely with a reservoir of bulk solution via a percolating liquid path to neighboring unfrozen pores or an external bath [46–50]. In this scenario, the liquid electrolyte and any solid ice within the pore remain at quasiequilibrium with the bulk reservoir at a constant chemical potential. The connected path to the reservoir may pass through liquid-saturated pores or partially frozen pores with sufficiently thick liquid films to allow unhindered transport.

As freezing proceeds, many ions and water molecules will inevitably be trapped out of *global* equilibrium, although still at *local* quasiequilibrium within each nanoscale pore. The simplest case is that of a pore connected to an external reservoir only via a bottleneck, sketched in Fig. 1(b). Water molecules that are not closely associated with ions can still go through the bottleneck, with a possibly different viscosity. The bottleneck may block solvated ions (with their solvation shells) from passing by steric hindrance or charge exclusion. Even if some solvated ions can diffuse through a given bottleneck, their electrokinetic transport rate may be too slow to allow many to escape prior to more complete freezing [51–53]. Such slow ion transport may be enhanced by long, tortuous pathways through a series of bottlenecks [54–57] and compounded by a large volume of micropores, effectively cut off from the macropores with insufficient time for salt release, in materials of low pore-space accessivity [50]. Even in relatively well-connected porous structures, nanofluidic salt trapping can also result from bottlenecks created by the advancing ice, as shown in Fig. 1(c), where the larger open pore on the right side freezes almost completely first. Due to the surface hydrophilicity, a supercooled liquid film often remains between the pore surface and the ice core prior to complete freezing [11,16,58], which is now the only pathway for water and ions in the

smaller pore shown on the left side. As the temperature decreases further, ice formation starts in the left pore, but transport of solvated ions through the thin liquid film is now slow, and the entropy of these confined ions builds up a pressure. In biological cells, as shown in Fig. 1(d), electrolytes are contained within the cell walls, and nanofluidic salt trapping is facilitated by the charged cytoskeleton and abundant charged macromolecules (including cryoresistant proteins). Internal salt concentrations are also actively maintained by ion channels and pumps in the cell membrane [59].

To quantitatively calculate the time scales of freezing and ion transport, one needs to solve a proper electrokinetic model of the three-dimensional charged pore structure, with information on the tortuosity and connectivity in addition to the pore sizes. Here we assume the asymptotic behavior of a very long ion transport time scale vs a freezing time scale, which is hereafter referred to as the limit of trapped ions. The phenomenon of ion trapping in charged nanochannels, while water remains free to diffuse and flow to a nearby reservoir or larger pore, is well established in the field of nanofluidics and forms the basis for various devices, such as electro-osmotic micropumps [60], nanofluidic diodes and bipolar transistors [54,61,62], and nanofluidic ion separators [63].

The supercooling of confined liquids can be greatly enhanced by the salt rejected by freezing, as the remaining solution becomes more concentrated inside a trapped freezing pore. High disjoining pressures are then produced in the very concentrated liquid solution and transmitted to the solid matrix, potentially causing damage.

At sufficiently low temperatures, salt-enhanced supercooling and freeze-thaw pressure are relieved by the sudden precipitation of ions from the concentrated liquid, thus allowing complete freezing of the pores. Ions may also be cleared by adsorption reactions on the pore surface, which regulate and neutralize the surface charge.

II. THEORY

As mentioned above, under the assumption of separated time scales for ion transport and freezing, we approximate the dynamic problem as a quasiequilibrium problem: in the limit of free ions, ion and water transport is much faster than freezing; in the other limit of trapped ions, ion transport is much slower than freezing. The solutions of both limits can be unified in the same quasiequilibrium mean-field framework. Below we present details of these solutions.

The mean-field free energy for a liquid electrolyte and its frozen solid inside a charged pore can be described by

$$\begin{aligned}
 F_{\text{tot}} &= F_{\text{liquid}} + F_{\text{solid}} + F_{\text{interface}} \\
 &= \int_{V_s} dV \left(\mu_s - \mu_l - \frac{\epsilon_s}{2} \|\vec{\nabla}\phi\|^2 \right) + \int_{V_l} dV \left[g(\{c_i\}) + \rho\phi - \frac{\epsilon_l}{2} \|\vec{\nabla}\phi\|^2 \right] \\
 &\quad + \sum_{j=s,l,sl} \int_{S_j} dS (\gamma_j + q_j\phi),
 \end{aligned} \tag{1}$$

where the integrations are performed over volumes of solid (V_s) and liquid (V_l) with permittivities ϵ_s and ϵ_l , respectively, and over surfaces of the solid-liquid interface (S_{sl}), the liquid-pore interface (S_l) and the solid-pore interface (S_s), with corresponding surface charge densities, q_{sl} , q_l , and q_s , and interfacial tensions, γ_{sl} , γ_l , and γ_s ; $\mu_s - \mu_l$ is the bulk chemical potential difference between solid and liquid phases; $-\vec{\nabla}\phi$ is the electric field; $g(\{c_i\})$ the nonelectric part of homogeneous liquid electrolyte free energy; c_i the concentration of ion species i having charge $z_i e$; and $\rho = \sum_i z_i e c_i$ the net charge density, assumed to be negligible in the solid phase. We focus on situations of complete wetting by the liquid, $\gamma_s - \gamma_l \gg \gamma_{sl}$, in which case we can neglect S_s and assume that S_l covers the entire pore surface.

Setting $\delta F_{\text{tot}}/\delta\phi = 0$ for bulk and surface variations, we obtain Poisson's equation,

$$\epsilon_l \nabla^2 \phi = -\rho \quad \text{in } V_l, \quad \epsilon_s \nabla^2 \phi = 0 \quad \text{in } V_s, \tag{2}$$

and electrostatic boundary conditions,

$$q_{sl} = (\epsilon_s \vec{E}_s - \epsilon_l \vec{E}_l) \cdot \hat{n}_{ls} \quad \text{on } S_{sl}, \quad q_l = \epsilon_l \vec{\nabla} \phi \cdot \hat{n}_l \quad \text{on } S_l. \quad (3)$$

The equilibrium state of liquid-solid coexistence is found by minimizing the total free energy with respect to the position and shape of the solid-liquid interface, S_{sl} . Here, we consider two cases: (i) an open pore where ions of species i exchange freely with a reservoir of concentration c_i^∞ and (ii) a pore with trapped ions, whose total number is fixed by screening the pore surface charge in the liquid, prior to freezing, by the mechanisms shown in Fig. 1. Importantly, we neglect the effects of volume changes due to the water/ice transformation, under the assumption that liquid water molecules (of size ~ 3 Å) are mobile and small enough to escape the pore as freezing progresses, regardless of whether solvated ions are trapped. In contrast to the common wisdom about freeze-thaw damage in pavements, this picture must also hold for well-connected hierarchical porous materials such as concrete.

The preceding thermodynamic framework for confined electrolyte phase transformations can be extended in various ways, e.g., to account for ion-ion correlations [64] (especially involving multivalent ions), finite ion sizes [65], and hydration surface forces [66,67], but here we focus on the simplest PB mean-field theory [31], which suffices to predict the basic physics of freezing point depression and material damage. The homogeneous free energy is then given by the ideal-gas entropy for pointlike ions, $g_i = c_i [\ln(v_i c_i) - 1]$, with v_i the molecular volume, and the electrostatic potential in the liquid electrolyte is then given by the PB equation:

$$-\epsilon_l \nabla^2 \phi_l = \rho = \sum_i z_i e c_i, \quad c_i = c_i^\infty e^{-\beta z_i e \phi_l}. \quad (4)$$

Since we focus on highly confined electrolyte liquid films, we set the relative permittivity, $\epsilon_l = 10\epsilon_0$, to that of water near dielectric saturation at a high charge density [68,69].

To assess the prevalence of nanofluidic salt trapping within PB theory, the state of a bottleneck shown in Fig. 1 can be estimated by comparing the double-layer thickness λ_D (or hydrated ion size a) inside with its radius R : if $\lambda_D \sim R$ (or $a \gtrsim R$), then the double layer(s) spans across and the bottleneck is approximated as “closed” to ions, since the freezing rate may exceed the ion transport rate, given a high tortuosity of the pore network. If $\lambda_D \ll R$ (or $a \lesssim R$), then the channel may be viewed as open to ion exchange. For an initial salt concentration of 0.1 M in a binary monovalent electrolyte (with relative permittivity $\epsilon_r \sim 10$), we find $\lambda_D \sim \sqrt{\frac{4\pi\epsilon_l k_B T}{2c_0 e^2}} \sim 0.5$ nm.

A. Symmetric pores

In order to obtain analytical results, we consider isotropic electrolyte freezing in d dimensions, where ice nucleates to form a plate ($d = 1$), cylinder ($d = 2$), or sphere ($d = 3$) of radius r within a pore of the same symmetry, whose surface is located at $x = R$. The total pore volume is $V(d)r^d$, and $S(d)r^{d-1}$ is the surface area of the ice core ($x < r$), surrounded by a liquid electrolyte shell ($r < x < R$). At thermodynamic equilibrium, the location r^* of the solid-liquid interface is determined by minimizing the total free energy with respect to r , $\delta F_{\text{tot}}/\delta r = 0$,

$$r^* = \text{argmin}_r F_{\text{tot}}(r), \quad (5)$$

which yields the equilibrium ice volume fraction, $\chi = (r^*/R)^d$. Once r^* is found, the mechanical equilibrium at the solid-liquid interface gives the pressure of both phases, which is transmitted to the pore boundary:

$$P = -\left(\frac{\partial F_{\text{solid}}}{\partial r}\right)_{r=r^*} = \left(\frac{\partial F_{\text{liquid}}}{\partial r}\right)_{r=r^*}. \quad (6)$$

The first equality describes the tendency to form more ice and hence expand its volume, while the second equality shows the free energy cost to squeeze the electrolyte, resisting the growth of ice.

For a symmetric pore, after freezing starts, the free energy of ice is given by

$$F_{ice} = (\mu_s - \mu_l)V(d)r^d, \quad (7)$$

where $(\mu_s - \mu_l)$ is the Gibbs free energy change per volume for bulk water freezing, which can be calculated [58] using the Gibbs-Helmholtz relation, as shown in Ref. [70]. In principle, the electric field energy of the ice core ($x < r$) depends on its shape and the electrostatic boundary conditions but vanishes here by symmetry. The interfacial energy is $F_{\text{surface}} = \gamma_{sl}S(d)r^{d-1}$, which gives rise to the Gibbs-Thomson [71] effect of freezing point depression for confined pure water. The free energy of the electrolyte shell is given by

$$\frac{F_{\text{elec}}}{S(d)} = q_l\phi(R)R^{d-1} + \int_r^R x^{d-1} dx \left[g(\{c_i\}) + \rho\phi - \frac{\epsilon_l}{2} \|\vec{\nabla}\phi\|^2 \right], \quad (8)$$

where the first term is the electrostatic energy of surface charges, and the integrand takes the form given above for mean-field theory of pointlike ions. To summarize, we are solving a free boundary problem where the liquid-ice boundary position r is unknown beforehand. We adopt a numerical algorithm to search for the r that minimizes the total free energy at a given temperature T , surface charge density q , and initial salt concentration c_0 :

- (1) Starting from $r = 0$, compute the total free energy $F(0)$.
- (2) Increment r by a small amount, dr , and compute the total free energy $F(r)$.

When computing the total free energy at a given r value, we always solve the Poisson-Boltzmann equation, (4), to obtain the electric potential profile ϕ and insert it into the integration of Eq. (8).

(3) After sweep r from 0 to the pore size R , find the minimum of F and the corresponding r gives the position of the quasiequilibrium ice front.

B. Free ions

As freezing proceeds in an open pore, where all ions can escape to a reservoir, the surface charge is eventually screened in a thin liquid film containing only counterions, which corresponds to one-component plasma [72,73]. The PB equation for the one-component plasma can be integrated for symmetric pore shapes [70] to obtain the mean electrostatic potential. For a slit pore ($d = 1$), we obtain to first order

$$|\tilde{P}| \approx \frac{4\pi\epsilon_l k_B T_0 Z^2}{q^2 e^2} \left| Q \frac{\Delta T}{T_0} \right| \sqrt{\frac{|\tilde{P}|}{2}} \tan \left(\sqrt{\frac{|\tilde{P}|}{2}} \frac{Rq e^2}{4\pi\epsilon_l k_B T} \right) = 2\pi, \quad (9)$$

where Q is the latent heat of bulk water freezing, T_0 the bulk freezing point, and $\Delta T = T - T_0$ the freezing point depression. Note that for the one-component plasma limit, the total amount of counterions does not depend on the pore size but is simply determined by the surface charge density. Hence, the quasiequilibrium solution depends only on the distance between the ice front and the pore surface, which we here denote L .

Inserting typical values, we can estimate the freezing point depression in the slit pore as $\Delta T \sim 0.1$ K and the pressure as $P_{\text{elec}} \sim 0.1$ MPa. In this case, the freezing point is only depressed by $\lesssim 1$ K, and no significant pressure is generated, as shown in Fig. 2. As shown in Ref. [70], the effects of ions in open cylindrical ($d = 2$) or spherical ($d = 3$) pores are even smaller than in a slit pore ($d = 1$) and may often be neglected compared to the Gibbs-Thomson effect of interfacial tension in such curved geometries. In general, if excess salt ions (and water molecules) are free to escape the pore during freezing, then we expect very little freeze-thaw damage in a wet porous material.

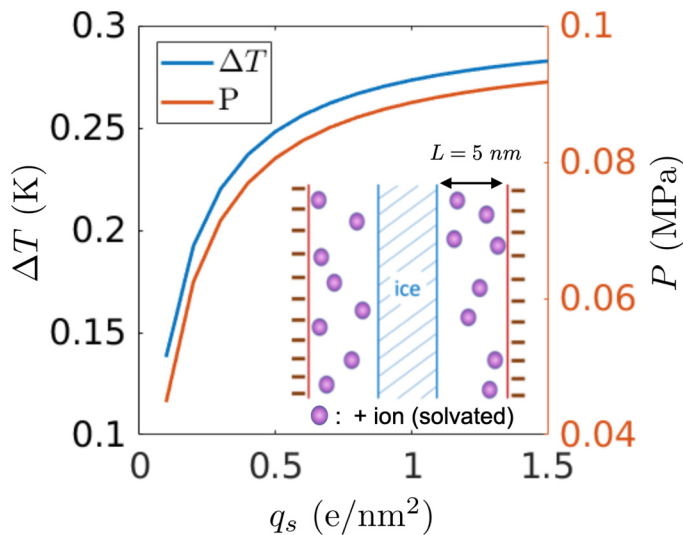


FIG. 2. Electrolyte freezing and pressure generation in a parallel-slit pore ($d = 1$) with *free* ions exchanging with a reservoir. There is no effects of interfacial tension. The freezing point depression, $\Delta T \sim 0.1$ K, and disjoining pressure, $P \sim 0.1$ MPa, are quite small, in the limit of one-component plasma of only counterions. In this case the total number of counterions is determined by the surface charge density only and does not depend on the pore size. And ΔT and P depend only on the distance between the ice front and the pore surface, which is denoted by $L = 5$ nm here.

C. Trapped ions

The situation is completely different in the opposite limit, where all ions in the original liquid binary electrolyte remain trapped within the pore during freezing. Total ion number conservation is then imposed on the PB equations, $\int_r^R c_i S(d)x^{d-1} dx = N_i$, and significant freezing point depression can be achieved. The mathematical details can be found in a companion paper [70], and here we focus on explaining the physical predictions of the theory. To separate the effect of curvature, here we focus on the slit symmetry ($d = 1$).

First, we consider a binary 1:1 liquid electrolyte freezing in a parallel-slit pore ($d = 1$). In this case, there is no effect of solid-liquid interfacial tension, as the interface area does not change as the ice front advances (zero curvature). As shown in Fig. 3, the freezing point is substantially decreased by increasing the initial salt concentration c_0 in the confined liquid. After freezing starts at temperature T_f , due to the resistance of the electrolyte, the equilibrium ice volume fraction χ monotonically increases as the temperature decreases. The freezing process continues until the trapped ions are suddenly removed from the thin liquid film at the temperature of freezing finished T_{ff} , when the salt solubility limit is reached, and χ suddenly jumps to 1. The pore is completely frozen now. Complete freezing may also occur if the trapped ions are adsorbed on the pore surface, thereby neutralizing the surface charge (as shown below).

As shown in Fig. 4, significant disjoining pressures (~ 10 MPa for $R = 5$ nm) can be generated by confined ions during the freezing process. The pressures at the freezing start temperature T_f and the complete freezing temperature T_{ff} are labeled P_f and P_{ff} , respectively. The disjoining pressure varies approximately linearly with the temperature between these values during the freezing process in a slit pore.

D. Salt solubility limit and surface charge regulation

As the ice volume fraction increases, the salt concentration goes up. At some point the concentrated electrolyte will become saturated and the salt will crystallize. The volume of salt crystal

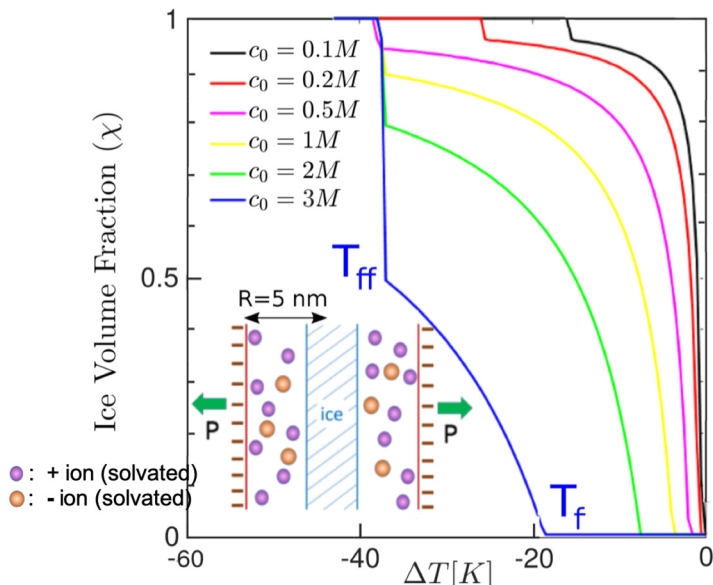


FIG. 3. In contrast to Fig. 2, for a binary electrolyte with *trapped* ions, a freezing point depression as large as -40 K can occur. The quasiequilibrium approximation gives a continuous freezing temperature range marked by two T values: the temperature to start freezing, T_f , and that of complete freezing of the pore, T_{ff} , when ions are removed by precipitation.

precipitate is neglected. The solubility equilibrium for 1:1 electrolyte ($M^+ + B^-$) at saturation is $K_{eq} = \frac{[M^+][B^-]}{[MB]} = \left(\frac{c_0^{\text{sat}}}{c_{\text{solid}}}\right)^2$. Here c_{solid} is the concentration in the solid crystal phase, which is typically regarded as a constant 1. Once c_0^{sat} , the saturated concentration of salt ions, is reached the equilibrium position of the ice front becomes thermodynamically unstable and all the liquid turns into solid phases of ice and salt crystal. In Fig. 3, all the curves at some point reach the solubility limit and undergo sudden crystallization, when the ice volume fraction discontinuously jumps from $\chi < 1$ to $\chi = 1$. The pressure at this point is denoted P_{ff} in both Fig. 4 and Fig. 5. As opposed to the concept of “crystallization pressure” [22,23], which has been proposed to account for pressure and damage (under room temperature) in construction materials, here the pressure of

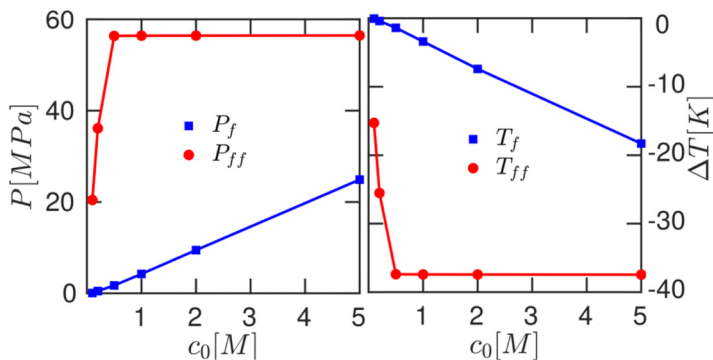


FIG. 4. High disjoining pressures, up to ~ 10 MPa, occur during the freezing process, below the temperature to start freezing, T_f , and above that of complete freezing of the pore, T_{ff} . The range of pressure is marked by P_f and P_{ff} , correspondingly. Blue squares and red circles show numerical results, while solid lines connecting them are a guide for the eyes.

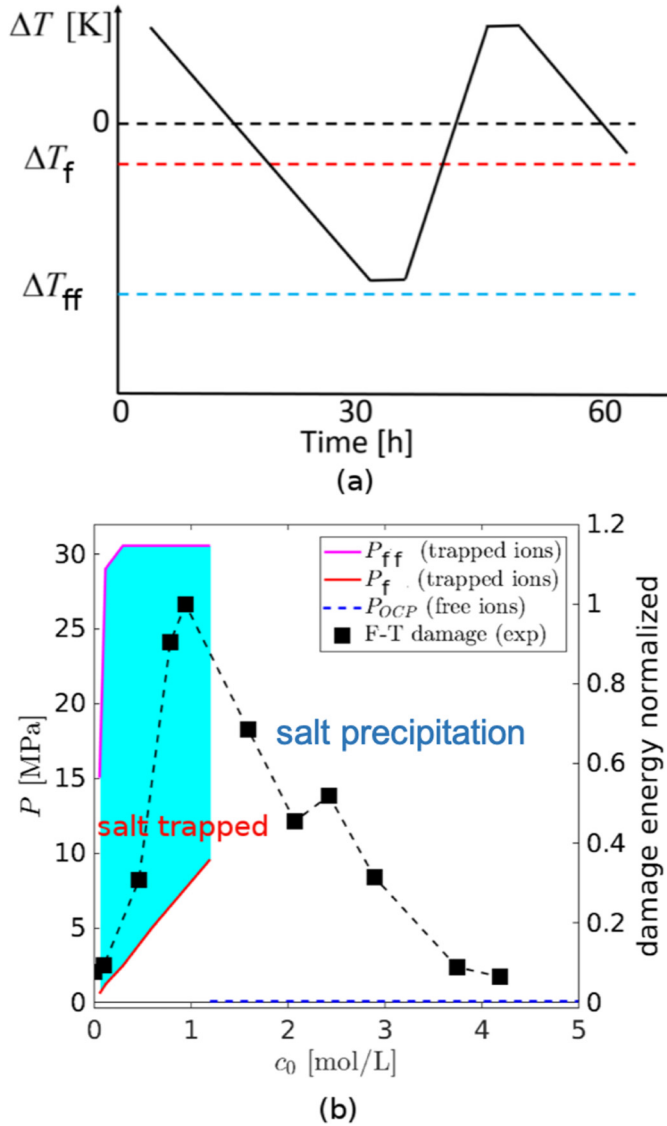


FIG. 5. (a) Typical experiment protocol reproduced from [24]. T_f and T_{ff} correspond to the temperature where ice formation is initiated and the solubility limit reached, as indicated in Fig. 3. (b) The shaded area shows the pressure range after freezing starts in a trapped pore. P_f and P_{ff} correspond to the pressure where ice formation is initiated and the solubility limit reached, as indicated in Fig. 4. The dashed line shows open pores with free ions, which is close to the horizontal line of 0. Data points show the measured damage in the cement paste FT experiment [24], a nonmonotonic function of the salt concentration. The tensile strength of hardened cement paste is ~ 3 MPa. (a) cement FT experiment protocol and (b) predicted pressure ranges compared with damage measurement.

the freezing pore is determined by thermodynamic equilibrium between freezing and precipitation, thus salt crystallization is merely a consequence, instead of the cause, of pressure.

When the concentration of trapped ions is high enough, counterion recombination with the surface charge becomes important. This effect can be included by a modified boundary condition for the PB equations, where the surface charge is computed self-consistently based on a charge regulation model [74] (see more details in [70]).

III. APPLICATION TO CONCRETE

The predictions of this theory are semiquantitatively consistent with experimental observations of freeze-thaw damage in cement. Below the critical degree of water saturation, plenty of large pores remain open transport pathways for ions during freezing, hence no significant damage is observed [25]. The volume expansion of water during freezing is irrelevant in this theory, so it can also explain the qualitatively similar results observed in freeze-thaw experiments on cement samples loaded with benzene, which shrinks upon freezing [21]. It is noted that the expansion reported in Ref. [21] is much smaller than the typical expansion caused by water freezing, hence more detailed investigation of benzene-loaded systems may help to clarify this scenario. The nonmonotonic dependence of the damage on the NaCl concentration [24] can be explained by crossover from salt trapping to channel opening through charge regulation, as shown in Fig. 5. A fully quantitative comparison requires the plasticity and fracture mechanics of the solid matrix due to these local high pressures and the connectivity of the pores, which is currently a missing link. Also, to quantify the transport time scales for ions as freezing proceeds, pore connectivity is key information. Nevertheless, to our knowledge, for the first time this mechanism shows the potential to encompass all these observations. This work may complement engineering models for cement FT such as that in [75].

IV. DISCUSSION AND CONCLUSIONS

In this article, we present a theory of the freezing of electrolytes in charged porous media. The key insight is that if ions become trapped by the advancing ice front, high disjoining pressures can cause material damage, until further supercooling triggers salt precipitation and complete freezing. The freezing point depression, ice volume fraction, and pressure are calculated using a simple mean-field theory.

Many extensions of the theory could be considered in future work. Ion correlations, including the strong-coupling limit [76–78], can be introduced via higher-order terms in Eq. (8), resulting in modified PB equations [64]. At larger length scales, models of interfacial instabilities leading to dendritic growth [79–81] could be extended to account for electrokinetic phenomena in charged pores [82,83]. Here we always assume that the bulk phase of ice (the I_h phase) is formed, since the freezing conditions discussed here ($T > 200$ K, $P < 100$ MPa, $d < 100$ nm) are not very extreme. Exotic phases of ice (non- I_h phases) are known to dominate under more extreme conditions [9,84–89]. Salt ions can also affect the surface tension of the ice-electrolyte interface, as well as other aspects of nucleation under confinement, described in a companion paper [70]. The effect of salt on the solution viscosity is neglected here but has been discussed in, e.g., [90,91].

As a first application to material durability, our theory is consistent with complex trends of freeze-thaw damage in hardened cement paste. These predictions could influence industrial practices in road deicing and pavement design. The theory may also provide some perspective on the physics of cryotolerance and cryopreservation in biological materials, which abound in electrolyte-soaked macromolecules, nanopores, and membranes.

ACKNOWLEDGMENTS

The authors thank S. Yip, C. Qiao, J. Weiss, and M. Pinson for useful discussions. This work was carried out with the support of the Concrete Sustainability Hub at MIT.

-
- [1] C. L. Guy, Cold acclimation and freezing stress tolerance: Role of protein metabolism, *Annu. Rev. Plant Biol.* **41**, 187 (1990).
 - [2] J. Saragusty and A. Arav, Current progress in oocyte and embryo cryopreservation by slow freezing and vitrification, *Reproduction* **141**, 1 (2011).

- [3] J. M. Storey and K. B. Storey, Physiology, biochemistry, and molecular biology of vertebrate freeze tolerance: The wood frog, in *Life in the Frozen State* (CRC Press, Boca Raton, FL, 2004), pp. 269–300.
- [4] C. J. Andrews, How do plants survive ice? *Ann. Bot.* **78**, 529 (1996).
- [5] F. F. Abdel Hafez, N. Desai, A. M. Abou-Setta, T. Falcone, and J. Goldfarb, Slow freezing, vitrification and ultra-rapid freezing of human embryos: a systematic review and meta-analysis, *Reprod. BioMed. Online* **20**, 209 (2010).
- [6] R. Wakchaure, S. Ganguly, S. Sharma, P. K. Praveen, M. Sharma, and T. Mahajan, A review on cryopreservation of embryos and its research implications in animal breeding and reproduction, *Int. J. Pharm. Biomed. Res.* **2**, 11 (2015).
- [7] L. Rienzi, C. Gracia, R. Maggiulli, A. R. LaBarbera, D. J. Kaser, F. M. Ubaldi, S. Vanderpoel, and C. Racowsky, Oocyte, embryo and blastocyst cryopreservation in art: Systematic review and meta-analysis comparing slow-freezing versus vitrification to produce evidence for the development of global guidance, *Hum. Reprod. Update* **23**, 139 (2017).
- [8] O. Mishima and H. E. Stanley, The relationship between liquid, supercooled and glassy water, *Nature* **396**, 329 (1998).
- [9] C. A. Tulk, C. J. Benmore, J. Urquidi, D. D. Klug, J. Neufeind, B. Tomberli, and P. A. Egelstaff, Structural studies of several distinct metastable forms of amorphous ice, *Science* **297**, 1320 (2002).
- [10] P. G. Debenedetti, Supercooled and glassy water, *J. Phys.: Condens. Matter* **15**, R1669 (2003).
- [11] L. D. Gelb, K. E. Gubbins, R. Radhakrishnan, and M. Sliwiska-Bartkowiak, Phase separation in confined systems, *Rep. Prog. Phys.* **62**, 1573 (1999).
- [12] D. T. Limmer and D. Chandler, Phase diagram of supercooled water confined to hydrophilic nanopores, *J. Chem. Phys.* **137**, 044509 (2012).
- [13] K. Morishige and H. Iwasaki, X-ray study of freezing and melting of water confined within SBA-15, *Langmuir* **19**, 2808 (2003).
- [14] M. Nosonovsky and B. Bhushan, Phase behavior of capillary bridges: Towards nanoscale water phase diagram, *Phys. Chem. Chem. Phys.* **10**, 2137 (2008).
- [15] K. V. Agrawal, S. Shimizu, L. W. Draushuk, D. Kilcoyne, and M. S. Strano, Observation of extreme phase transition temperatures of water confined inside isolated carbon nanotubes, *Nat. Nanotechnol.* **12**, 267 (2017).
- [16] P. A. Bonnaud, B. Coasne, and R. J. M. Pellenq, Molecular simulation of water confined in nanoporous silica, *J. Phys.: Condens. Matter* **22**, 284110 (2010).
- [17] S. Cerveny, F. Mallamace, J. Swenson, M. Vogel, and L. Xu, Confined water as model of supercooled water, *Chem. Rev.* **116**, 7608 (2016).
- [18] Y. Farnam, D. Bentz, A. Sakulich, D. Flynn, and J. Weiss, Measuring freeze and thaw damage in mortars containing deicing salt using a low-temperature longitudinal guarded comparative calorimeter and acoustic emission, *Adv. Civil Eng. Mater.* **3**, 316 (2014).
- [19] H. Cai and X. Liu, Freeze-thaw durability of concrete: ice formation process in pores, *Cem. Concr. Res.* **28**, 1281 (1998).
- [20] Portland Cement Association, Freeze-thaw resistance (2018), <https://www.cement.org/Learn/concrete-technology/durability/freeze-thaw-resistance>.
- [21] J. J. Beaudoin and C. MacInnis, The mechanism of frost damage in hardened cement paste, *Cem. Concr. Res.* **4**, 139 (1974).
- [22] E. M. Winkler and P. C. Singer, Crystallization pressure of salts in stone and concrete, *Geol. Soc. Am. Bull.* **83**, 3509 (1972).
- [23] M. Steiger, Crystal growth in porous materials—I: The crystallization pressure of large crystals, *J. Cryst. Growth* **282**, 455 (2005).
- [24] Y. Farnam, D. Bentz, A. Hampton, and W. Weiss, Acoustic emission and low-temperature calorimetry study of freeze and thaw behavior in cementitious materials exposed to sodium chloride salt, *Transport. Res. Record: J. Transport. Res. Board* **2441**, 81 (2014).
- [25] W. Li, M. Pour-Ghaz, J. Castro, and J. Weiss, Water absorption and critical degree of saturation relating to freeze-thaw damage in concrete pavement joints, *J. Mater. Civil Eng.* **24**, 299 (2011).
- [26] J. S. Wettlaufer and M. G. Worster, Premelting dynamics, *Annu. Rev. Fluid Mech.* **38**, 427 (2006).

- [27] T. Zhou, K. Ioannidou, E. Masoero, M. Mirzadeh, R. J.-M. Pellenq, and M. Z. Bazant, Capillary stress and structural relaxation in moist granular materials, *Langmuir* **35**, 4397 (2019).
- [28] T. Zhou, K. Ioannidou, F.-J. Ulm, M. Z. Bazant, and R. J.-M. Pellenq, Multiscale poromechanics of wet cement paste, *Proc. Natl. Acad. Sci. USA* **116**, 10652 (2019).
- [29] J. Lyklema, *Fundamentals of Interface and Colloid Science. Vol. II: Solid-Liquid Interfaces* (Academic Press, San Diego, CA, 1995).
- [30] J. N. Israelachvili, *Intermolecular and Surface Forces* (Academic Press, New York, 2011).
- [31] D. Andelman, Electrostatic properties of membranes: The Poisson-Boltzmann theory, in *Handbook of Biological Physics* (Elsevier, Amsterdam, 1995), pp. 603–641.
- [32] R. J.-M. Pellenq and H. Van Damme, Why does concrete set?: The nature of cohesion forces in hardened cement-based materials, *MRS Bull.* **29**, 319 (2004).
- [33] R. J.-M. Pellenq, J. M. Caillol, and A. Delville, Electrostatic attraction between two charged surfaces: A (n, v, t) Monte Carlo simulation, *J. Phys. Chem. B* **101**, 8584 (1997).
- [34] C. Alba-Simionesco, B. Coasne, G. Dosseh, G. Dudziak, K. E. Gubbins, R. Radhakrishnan, and M. J. P. C. M. Sliwinska-Bartkowiak, Effects of confinement on freezing and melting, *J. Phys.: Condens. Matter* **18**, R15 (2006).
- [35] K.-M. Jan and S. Chien, Role of surface electric charge in red blood cell interactions, *J. Gen. Physiol.* **61**, 638 (1973).
- [36] J. Visser, Adhesion of colloidal particles, in *Surface and Colloid Science*, edited by E. Matijevic (John Wiley and Sons, New York, 1973), Vol. 8, p. 3.
- [37] R. F. Giese, Interlayer bonding in kaolinite, dickite and nacrite, *Clays Clay Miner.* **21**, 145 (1973).
- [38] S. McLaughlin, Electrostatic potentials at membrane-solution interfaces, in *Current Topics in Membranes and Transport, Vol. 9* (Elsevier, Amsterdam, 1977), pp. 71–144.
- [39] S. L. Swartzen-Allen and E. Matijevic, Surface and colloid chemistry of clays, *Chem. Rev.* **74**, 385 (1974).
- [40] A. J. Allen, J. J. Thomas, and H. M. Jennings, Composition and density of nanoscale calcium–silicate–hydrate in cement, *Nat. Mater.* **6**, 311 (2007).
- [41] R. J.-M. Pellenq, A. Kushima, R. Shahsavari, K. J. Van Vliet, M. J. Buehler, S. Yip, and F.-J. Ulm, A realistic molecular model of cement hydrates, *Proc. Natl. Acad. Sci. USA* **106**, 16102 (2009).
- [42] A. Delville, N. Gasmı, R. J. M. Pellenq, J. M. Caillol, and H. Van Damme, Correlations between the stability of charged interfaces and ionic exchange capacity: A Monte Carlo study, *Langmuir* **14**, 5077 (1998).
- [43] R. Jellander, S. Marčelja, and J. P. Quirk, Attractive double-layer interactions between calcium clay particles, *J. Colloid Interface Sci.* **126**, 194 (1988).
- [44] J. Stankovich and S. L. Carnie, Electrical double layer interaction between dissimilar spherical colloidal particles and between a sphere and a plate: Nonlinear Poisson-Boltzmann theory, *Langmuir* **12**, 1453 (1996).
- [45] J. P. Valleau and L. K. Cohen, Primitive model electrolytes. I. Grand canonical Monte Carlo computations, *J. Chem. Phys.* **72**, 5935 (1980).
- [46] S. Torquato, *Random Heterogeneous Materials: Microstructure and Macroscopic Properties, Vol. 16* (Springer Science & Business Media, New York, 2013).
- [47] J. Van Brakel, Pore space models for transport phenomena in porous media review and evaluation with special emphasis on capillary liquid transport, *Powder Technol.* **11**, 205 (1975).
- [48] J. A. Quiblier, A new three-dimensional modeling technique for studying porous media, *J. Colloid Interface Sci.* **98**, 84 (1984).
- [49] M. B. Pinson, T. Zhou, H. M. Jennings, and M. Z. Bazant, Inferring pore connectivity from sorption hysteresis in multiscale porous media, *J. Colloid Interface Sci.* **532**, 118 (2018).
- [50] Z. Gu and M. Z. Bazant, Microscopic theory of capillary pressure hysteresis based on pore-space accessibility and radius-resolved saturation, *Chem. Eng. Sci.* **196**, 225 (2019).
- [51] P. M. Biesheuvel and M. Z. Bazant, Analysis of ionic conductance of carbon nanotubes, *Phys. Rev. E* **94**, 050601(R) (2016).
- [52] P. B. Peters, R. van Roij, M. Z. Bazant, and P. M. Biesheuvel, Analysis of electrolyte transport through charged nanopores, *Phys. Rev. E* **93**, 053108 (2016).

- [53] J. Catalano, R. G. H. Lammertink, and P. M. Biesheuvel, Theory of fluid slip in charged capillary nanopores, [arXiv:1603.09293](#).
- [54] G. Yossifon, I. Frankel, and T. Miloh, On electro-osmotic flows through microchannel junctions, *Phys. Fluids* **18**, 117108 (2006).
- [55] S. Pennathur and J. G. Santiago, Electrokinetic transport in nanochannels. 1. Theory, *Anal. Chem.* **77**, 6772 (2005).
- [56] H.-C. Chang, G. Yossifon, and E. A. Demekhin, Nanoscale electrokinetics and microvortices: How microhydrodynamics affects nanofluidic ion flux, *Annu. Rev. Fluid Mech.* **44**, 401 (2012).
- [57] G. Yossifon, P. Mushenheim, Y.-C. Chang, and H.-C. Chang, Nonlinear current-voltage characteristics of nanochannels, *Phys. Rev. E* **79**, 046305 (2009).
- [58] R. Denoyel and R. J. M. Pellenq, Simple phenomenological models for phase transitions in a confined geometry. 1: Melting and solidification in a cylindrical pore, *Langmuir* **18**, 2710 (2002).
- [59] H. Bertil, *Ionic Channels of Excitable Membranes* (Sinauer, Sunderland, MA, 1992).
- [60] S. Zeng, C.-H. Chen, J. C. Mikkelsen Jr., and J. G. Santiago, Fabrication and characterization of electroosmotic micropumps, *Sensors Actuat. B: Chem.* **79**, 107 (2001).
- [61] H. Daiguji, Y. Oka, and K. Shirono, Nanofluidic diode and bipolar transistor, *Nano Lett.* **5**, 2274 (2005).
- [62] G. Yossifon, Y.-C. Chang, and H.-C. Chang, Rectification, Gating Voltage, and Interchannel Communication of Nanoslot Arrays Due to Asymmetric Entrance Space Charge Polarization, *Phys. Rev. Lett.* **103**, 154502 (2009).
- [63] D. Gillespie and S. Pennathur, Separation of ions in nanofluidic channels with combined pressure-driven and electro-osmotic flow, *Anal. Chem.* **85**, 2991 (2013).
- [64] M. Z. Bazant, B. D. Storey, and A. A. Kornyshev, Double Layer in Ionic Liquids: Overscreening Versus Crowding, *Phys. Rev. Lett.* **106**, 046102 (2011).
- [65] M. Z. Bazant, M. S. Kilic, B. D. Storey, and A. Ajdari, Towards an understanding of nonlinear electrokinetics at large voltages in concentrated solutions, *Adv. Colloid Interface Sci.* **152**, 48 (2009).
- [66] K. Bohinc, A. Shrestha, M. Brumen, and S. May, Poisson-Helmholtz-Boltzmann model of the electric double layer: Analysis of monovalent ionic mixtures, *Phys. Rev. E* **85**, 031130 (2012).
- [67] M. A. Brown, G. V. Bossa, and S. May, Emergence of a stern layer from the incorporation of hydration interactions into the Gouy-Chapman model of the electrical double layer, *Langmuir* **31**, 11477 (2015).
- [68] F. Booth, The dielectric constant of water and the saturation effect, *J. Chem. Phys.* **19**, 391 (1951).
- [69] M. Aguilera-Arzo, A. Andrio, V. M. Aguilera, and A. Alcaraz, Dielectric saturation of water in a membrane protein channel, *Phys. Chem. Chem. Phys.* **11**, 358 (2009).
- [70] T. Zhou, M. Mirzadeh, R. J.-M. Pellenq, and M. Z. Bazant, Theory of freezing point depression in charged porous media (unpublished).
- [71] J. W. Gibbs, On the equilibrium of heterogeneous substance, *Transactions of the Connecticut Academy of Sciences* (1875), Vol. 3, pp. 343–524.
- [72] S. G. Brush, H. L. Sahlin, and E. Teller, Monte Carlo study of a one-component plasma. I, *J. Chem. Phys.* **45**, 2102 (1966).
- [73] M. Baus and J.-P. Hansen, Statistical mechanics of simple Coulomb systems, *Phys. Rep.* **59**, 1 (1980).
- [74] T. Markovich, D. Andelman, and R. Podgornik, Charge regulation: A generalized boundary condition? *Europhys. Lett.* **113**, 26004 (2016).
- [75] H. S. Esmaeeli, Y. Farnam, D. P. Bentz, P. D. Zavattieri, and W. J. Weiss, Numerical simulation of the freeze-thaw behavior of mortar containing deicing salt solution, *Mater. Struct.* **50**, 96 (2017).
- [76] A. G. Moreira and R. R. Netz, Strong-coupling theory for counter-ion distributions, *Europhys. Lett.* **52**, 705 (2000).
- [77] R. R. Netz, Electrostatics of counter-ions at and between planar charged walls: From Poisson-Boltzmann to the strong-coupling theory, *Eur. Phys. J. E* **5**, 557 (2001).
- [78] L. Šamaj and E. Trizac, Wigner-crystal formulation of strong-coupling theory for counterions near planar charged interfaces, *Phys. Rev. E* **84**, 041401 (2011).
- [79] M. B. Hastings and L. S. Levitov, Laplacian growth as one-dimensional turbulence, *Physica D* **116**, 244 (1998).

- [80] W. W. Mullins and R. F. Sekerka, Morphological stability of a particle growing by diffusion or heat flow, *J. Appl. Phys.* **34**, 323 (1963).
- [81] W. W. Mullins and R. F. Sekerka, Stability of a planar interface during solidification of a dilute binary alloy, in *Dynamics of Curved Fronts* (Elsevier, Amsterdam, 1988), pp. 345–352.
- [82] M. Z. Bazant, J. Choi, and B. Davidovitch, Dynamics of Conformal Maps for a Class of Non-Laplacian Growth Phenomena, *Phys. Rev. Lett.* **91**, 045503 (2003).
- [83] M. Mirzadeh and M. Z. Bazant, Electrokinetic Control of Viscous Fingering, *Phys. Rev. Lett.* **119**, 174501 (2017).
- [84] L. G. Dowell and A. P. Rinfret, Low-temperature forms of ice as studied by x-ray diffraction, *Nature* **188**, 1144 (1960).
- [85] D. C. Steytler, J. C. Dore, and C. J. Wright, Neutron diffraction study of cubic ice nucleation in a porous silica network, *J. Phys. Chem.* **87**, 2458 (1983).
- [86] E. Mayer and A. Hallbrucker, Cubic ice from liquid water, *Nature* **325**, 601 (1987).
- [87] B. J. Murray, D. A. Knopf, and A. K. Bertram, The formation of cubic ice under conditions relevant to earth's atmosphere, *Nature* **434**, 202 (2005).
- [88] E. B. Moore and V. Molinero, Is it cubic? Ice crystallization from deeply supercooled water, *Phys. Chem. Chem. Phys.* **13**, 20008 (2011).
- [89] J. L. Finney, A. Hallbrucker, I. Kohl, A. K. Soper, and D. T. Bowron, Structures of High and Low Density Amorphous Ice by Neutron Diffraction, *Phys. Rev. Lett.* **88**, 225503 (2002).
- [90] R. P. Spragg, J. Castro, W. Li, M. Pour-Ghaz, P.-T. Huang, and J. Weiss, Wetting and drying of concrete using aqueous solutions containing deicing salts, *Cem. Concr. Compos.* **33**, 535 (2011).
- [91] Y. Farnam, S. Dick, A. Wiese, J. Davis, D. Bentz, and J. Weiss, The influence of calcium chloride deicing salt on phase changes and damage development in cementitious materials, *Cement and Concrete Composites* **64**, 1 (2015).